

Infrared Ocean Surface Emissivity Models

Nicholas R. Nalli

NOAA/NESDIS/STAR

College Park, Maryland, USA

2020 ISSI Team Meeting

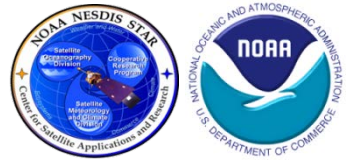
Dec 2020

- **Conventional Models**
 - Background and development
 - Criticality of surface-based FTS measurements
 - Observed underestimation of surface-leaving radiance
- **Operational Forward Modeling**
 - Modeling the surface-leaving radiance
 - CRTM Effective-Emissivity (IRSSE) Model approach
- **Current Topics of Ongoing Research**
 - Temperature dependence found in global data
 - Development and testing of temperature-dependent model
- **Summary and Future Work**

IR Ocean Emissivity Models

CONVENTIONAL MODELS

Background and Development



- For satellite IR remote sensing applications, the **surface emissivity** must be specified with a high degree of absolute accuracy
 - **0.5% uncertainty** $\Rightarrow \approx 0.3\text{--}0.4$ K systematic error in LWIR window channels
- Although models of IR sea-surface emission date back to the 1960s (e.g., *Saunders 1968*), it wasn't until the late 1980s that **IR emissivity models** would begin to gain traction, beginning with *Masuda et al. (1988)*, who published their calculations within a convenient lookup table (LUT)
- In these **conventional models**, emissivity is calculated as the ensemble-mean of one minus Fresnel reflectance of surface wave facets (e.g., *Masuda et al. 1988; Watts et al. 1996; Wu and Smith 1997; Masuda 2006*):

$$\begin{aligned} \bar{\epsilon}_\nu(\theta_0, N_\nu) &= 1 - \int_{\theta_n} \int_{\varphi_n} \rho_\nu(\theta_n, \varphi_n; \theta_0; N_\nu) P(\theta_n, \theta_0; \sigma_s^2) d\varphi_n d\mu_n \\ &= 1 - \bar{\rho}_\nu(\theta_0, N_\nu), \end{aligned}$$

Emissivity of Pure and Sea Waters for the Model Sea Surface in the Infrared Window Regions

K. MASUDA, T. TAKASHIMA, AND Y. TAKAYAMA

Meteorological Research Institute, Tsukuba, Ibaraki 305, Japan

Emissivity of pure and sea waters for the model sea surface is tabulated as a function of the zenith angle of observed radiation (θ) and the surface wind speed in the infrared window regions, 3.5–4.1 μm and 8–13 μm . The sea surface is simulated by many facets whose slopes are changed according to the isotropic Gaussian distribution with respect to surface wind. Emissivity is also computed for the plane surface condition. Computational results show that 1) emissivity decreases slowly with the increase of θ , 2) little effect of the surface wind is noted on emissivity for $\theta \leq 30^\circ$, whereas this effect greatly appears for $\theta > 70^\circ$, and 3) relative difference of emissivities between pure water and sea water is less than 0.1% within $\theta = 50^\circ$ for wind speed less than 15 m/s. Finally, the corresponding apparent temperatures are also examined.

1. Introduction

Recently sea surface temperature (SST) has been obtained in the infrared (IR) window region by high resolution multi-channel radiometer from space (Barton, 1983; Strong and McClain, 1984; Takashima and Takayama, 1986; et al.). The combined use of multiple spectral channels not only permits the simultaneous derivation of sea surface temperature with high accuracy but also affords atmospheric information as well. To further improve the accuracy of measurements of SST, the effect of emissivity on SST must appropriately be taken into account with respect to wavelength. Sea surface emissivity is affected by 1) surface roughness which in turn depends on surface wind, and 2) changes in the refractive index due to variation in salinity, chlorinity, and temperature. In addition, emissivity is a function of zenith angle of observed radiation.

In this paper, emissivity of the model sea surface within the infrared window regions is computed as a function of the

zenith angle of observed radiation and the surface wind speed. Comparisons of emissivity for pure water and that for sea water are also carried out. Further, apparent temperature differences due to the above emissivity differences are examined. This is an extended work of the previous paper by Takashima and Takayama (1981), where the case of pure water was considered.

2. Derivation of Equations

Emissivity from a plane water surface in thermodynamic equilibrium can be expressed by

$$\epsilon(n, \chi) = 1 - \rho(n, \chi), \quad (1)$$

where n , χ , and ρ are the complex refractive index of pure or sea water ($n = p - iq$), the angle of the emitted radiation with respect to the normal to the water surface and reflectance, respectively. The reflectance can be expressed in terms of n and the incident angle χ as

$$\rho(n, \chi) = (|\gamma_n|^2 + |\gamma_\perp|^2)/2, \quad (2)$$

Criticality of Surface-Based FTS Measurements



- While IR emissivity models have since gained widespread acceptance in operational satellite product systems, **this was only after they were empirically validated**
 - **Masuda’s model** was published in **1988, but it was not extensively used** because it was never validated against observations
 - Later models were improved to agree reasonably well with observations from the **Marine Atmospheric Emitted Radiance Interferometer (MAERI)** (Smith *et al.* 1996; Minnett *et al.* 2001), a ship-based Fourier transform spectrometer (FTS)
- As a result, IR emissivity has been all but taken for granted in many circles as a “solved problem”

Observations of the Infrared Radiative Properties of the Ocean—Implications for the Measurement of Sea Surface Temperature via Satellite Remote Sensing



William L. Smith,* R. O. Knuteson,* H. E. Revercomb,* W. Feltz,* H. B. Howell,* W. P. Menzel,* N. R. Nalli,* Otis Brown,* James Brown,* Peter Minnett,* and Walter McKeown*

(Minnett 1991). Another issue in the standard method of satellite SST validation is the physical difference between the surface skin temperature and the temperature observed from an oceanographic buoy at some depth (e.g., Robinson *et al.* 1984; Schuessel *et al.* 1987, 1990).

New high spatial and high spectral resolution radiometers [i.e., the Moderate Resolution Imaging Spectrometer (MODIS) and the Advanced Infrared Radiation Sounder (AIRS)] are being developed for the Earth Observing System (EOS) to improve the accuracy of SST determinations. However, before improvements can be realized, it is necessary to understand the physical variables contributing to sea surface emitted and reflected radiation to space. The emissivity of the ocean surface varies with view angle and sea state, the reflection of sky radiation also depends on view angle and sea state, and the absorption of atmospheric constituents such as water vapor, aerosols, and subvisible clouds affects transmittance.

To obtain a direct measure of the radiative properties of sea and atmospheric influences, an experimental field program was developed. The program deployed a University of Wisconsin (UW) high spectral resolution Atmospheric Emitted Radiance Interferometer (AERI) (see Revercomb *et al.* 1993) on the RV *Pelican* (Fig. 1), operated by the Louisiana Universities Marine Consortium (LUMCON). The AERI (Fig. 2) was configured to make spectral observations of the sea surface emitted radiance at several view angles along with the sky radiation reflected from the ocean (Fig. 3). In addition to the radiometric data, ocean salinity, intake water temperature and surface air temperature, humidity, and wind velocity were measured by the *Pelican*'s oceanographic and meteorological



FIG. 1. The *Pelican*, used to conduct the oceanographic experiments.

observing system. The Brookhaven National Laboratory provided an in situ “skimmer” SST device for measuring the temperature of the water within the top 15 cm of depth and a Heilmann broadband infrared radiation thermometer “window” radiometer for independent measurement of the radiative temperature of the sea surface at 10 μm . The UW launched radiometers from the ship on a routine schedule (i.e., approximately every 3 h). The Naval Research Laboratory provided measurements of the aerosol concentration of the marine boundary layer, a subject for a future paper. Techniques have been developed to infer the thermodynamic (rather than radiometric) temperature of the ocean skin from the AERI measurements, as well as the spectral distribution of the emissivity/reflectivity of the ocean surface. The cruise and measurements were conducted from 14 to 17 January 1995 in the northwestern Gulf of Mexico along



FIG. 2. The Atmospheric Emitted Radiance Interferometer aboard the *Pelican*.

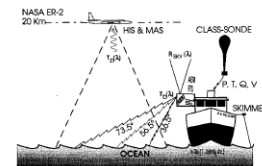
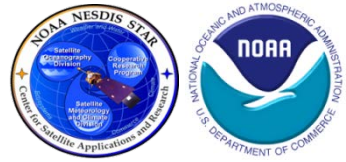


FIG. 3. Schematic illustrating the observations obtained during the *Pelican* cruise.



IR Ocean Emissivity Models

OPERATIONAL FORWARD MODELING

Considerations in Operational Forward Modelling



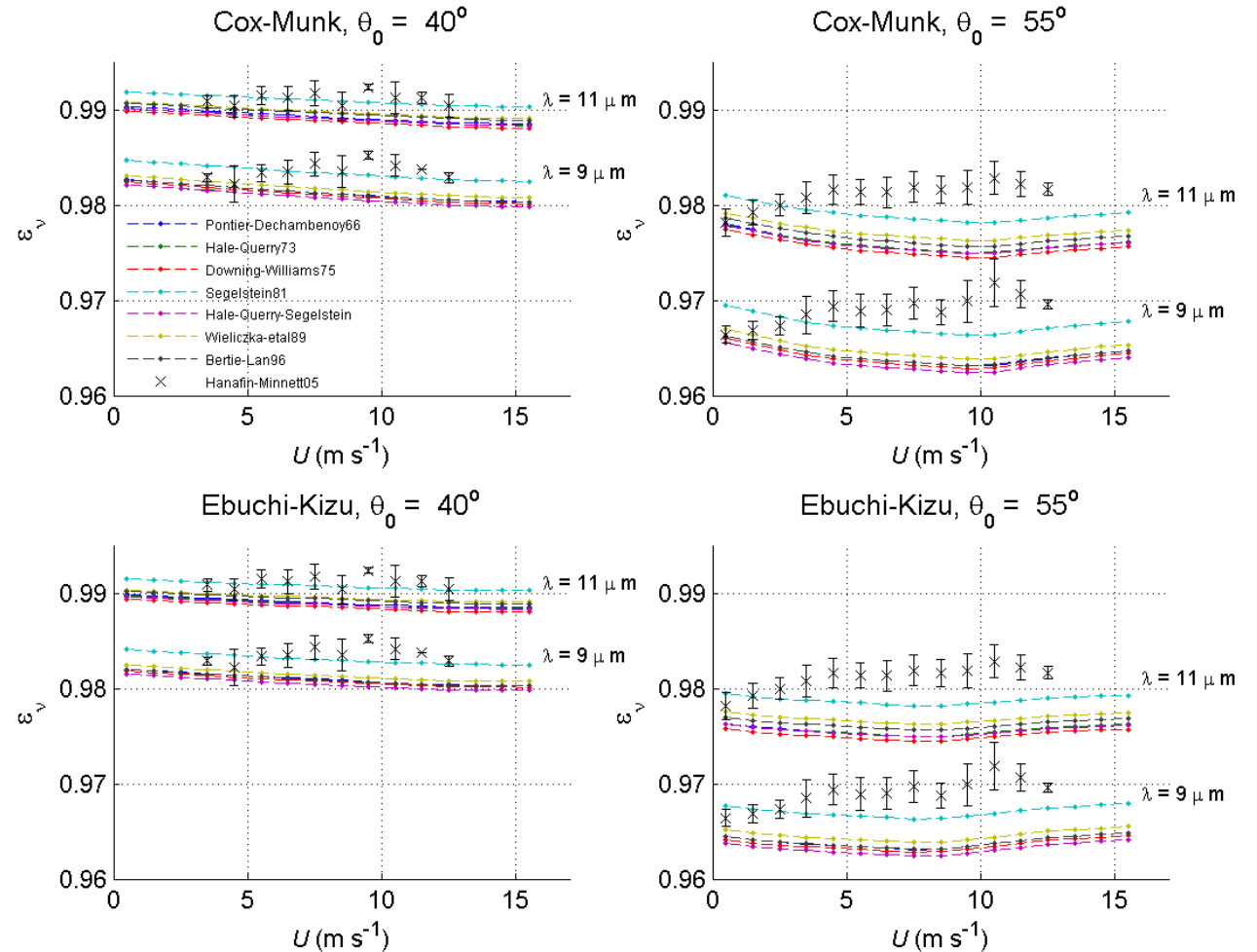
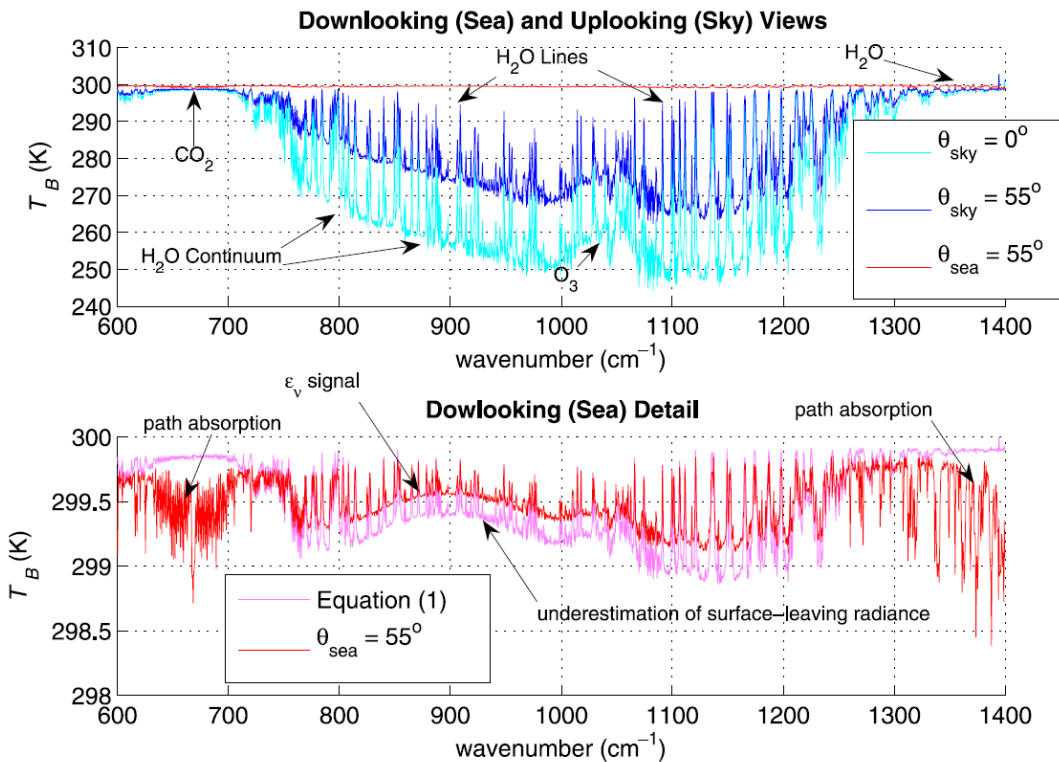
- In terms of the forward problem, it is the **IR surface-leaving radiance (SLR)** that we directly measure (**obs**)
- Therefore, it is this quantity that we ultimately need to model (**calc**)
- To achieve this, **both IR $\epsilon(\nu)$ and the BRDF** must be treated in a consistent manner so as not to violate energy conservation at the surface
- The BRDF is complicated by the fact that the downwelling IR radiance varies as a function of zenith angle
- It is thus **impractical** to perform an explicit case-by-case calculation of the full hemispheric BRDF; approximations must be employed
 - CRTM employs a specular approximation
 - SARTA employs a Lambertian approximation

Observed Underestimation of Surface-Leaving Radiance (SLR)



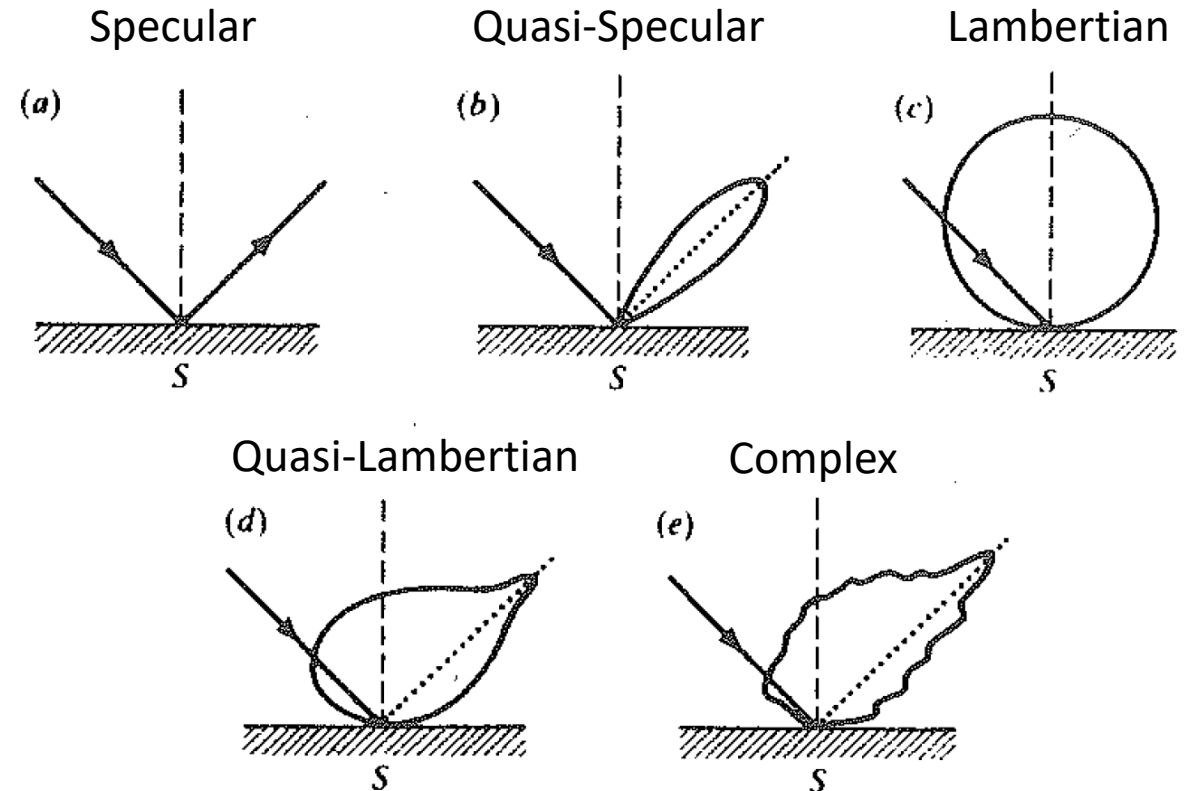
The specular approximation for SLR results in residual systematic discrepancies (0.1–0.4 K) at higher wind speeds and view angles $\geq 40^\circ$ (Nalli *et al.* 2001, 2006; Hanafin and Minnett 2005)

NALLI ET AL.: SHIP MEASUREMENTS FOR IR VALIDATION



The IR emissivity models are theoretically sound, so where's the culprit?

- **Approximation of multiple reflections**
 - Enhancement of emissivity in well-known analytical models includes only SESR radiation
 - Accounted for in Monte Carlo models (e.g., *Henderson et al. 2003*), or more complicated analytical models (e.g., *Bourlier 2006*), but less convenient to implement
 - Second order effect $\approx O(0.05)$ K
- **Incorrect specification of reflected atmospheric radiation**
 - The **ocean BRDF** is **quasi-specular**, i.e., diffuse with a large specular component (*Nalli et al. 2001; Watts et al. 1996*)
 - However, because of the impracticality associated with a **hemispheric double integral**, radiative transfer models typically treat the reflectance as **either specular or Lambertian**

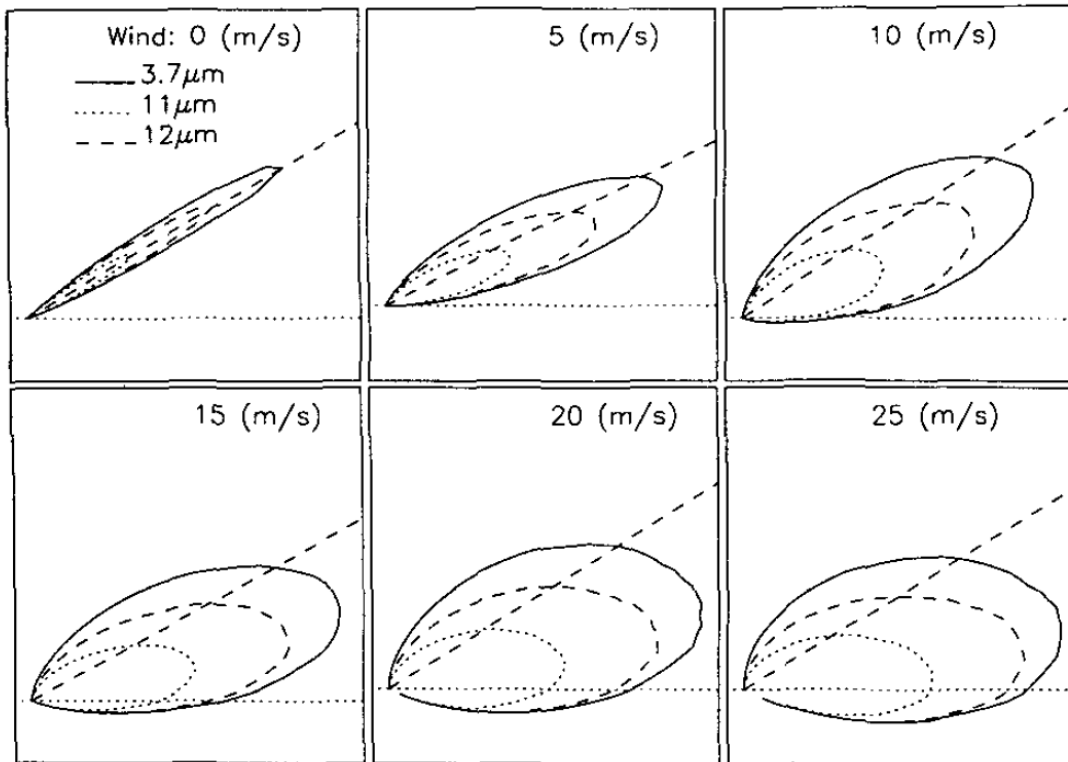


From Stephens (1994)

$$[1 - \bar{\epsilon}_\nu(\theta_0)] I_\nu^\downarrow(\theta_0) \equiv \bar{\rho}_\nu(\theta_0) I_\nu^\downarrow(\theta_0) < \iint \rho_\nu(\theta_n, \varphi_n; \theta_0) I_\nu^\downarrow(\theta) P(\theta_n, \theta_0; \sigma_s^2) d\varphi_n d\mu_n$$

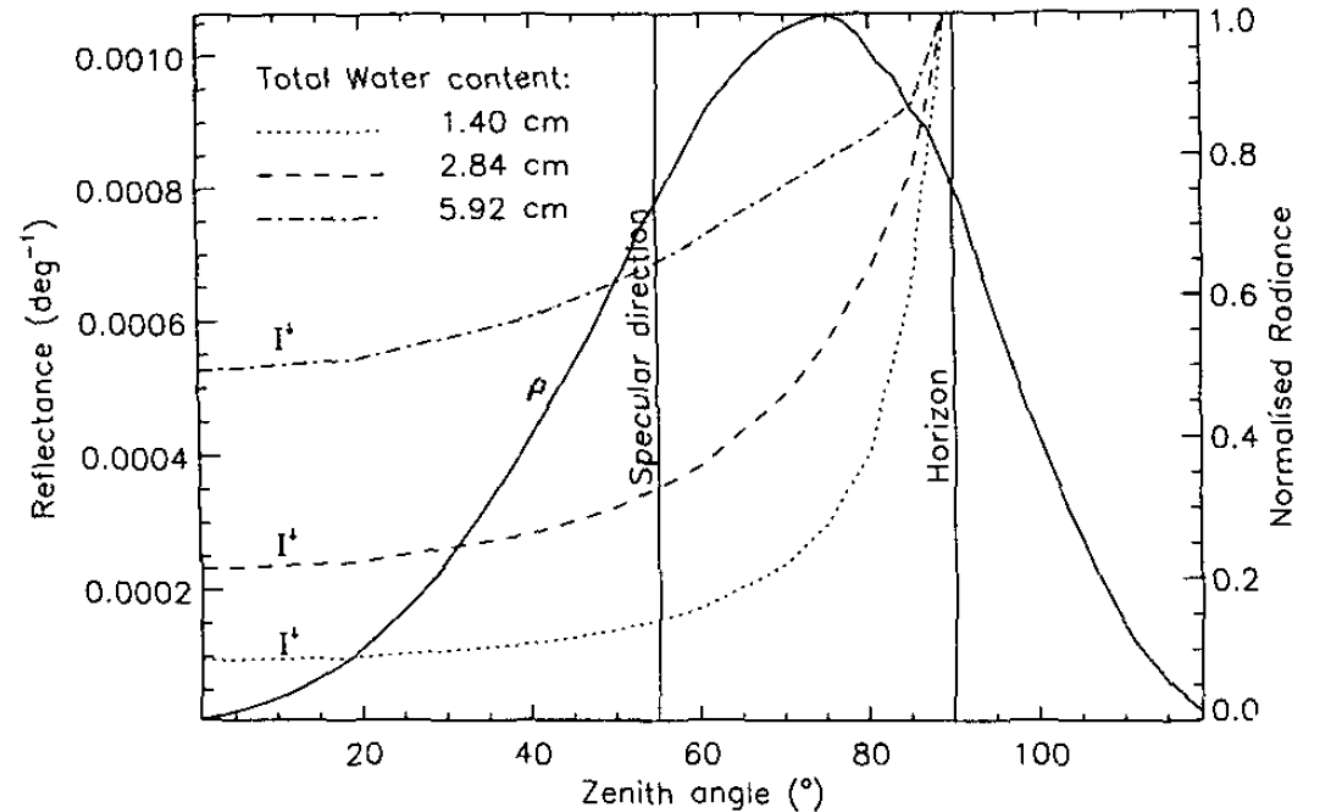
Quasi-Specular Reflection in the Infrared

Modeled Reflection Lobes
(Watts et al. 1996)



Surface Reflectivity and Downwelling Atmospheric Radiance as Function of Zenith Angle

(Watts et al. 1996)



Figures from Watts et al. (1996)

Radiative Transfer-Based Effective Emissivity

- A handful of previous investigators sought **practical solutions** to the **quasi-specular ocean BRDF problem** (*Watts et al. 1996; Nalli et al. 2001*), but these ultimately were not satisfactory for existing operational algorithms and models (e.g., CRTM)
- The **CRTM IR sea surface effective-emissivity (IRSSE) model** (*Nalli et al. 2018a,b; van Delst et al. 2009*) was thus derived to account for the quasi-specular ocean BRDF in a manner practical for **operational assimilation and retrievals**

The conical-directional reflectance for non-isotropic incident radiation (*Nicodemus et al. 1977*) for the sea surface reflectance

$$\rho_{\nu}(\theta_0, \sigma_s^2) = \frac{\iint \rho_{\nu}(\theta_n, \varphi_n; \theta_0) P(\theta_n, \theta_0; \sigma_s^2) [B_{\nu}(T_s) - I_{\nu}^{\downarrow}(\theta)] d\varphi_n d\mu_n}{\iint P(\theta_n, \theta_0; \sigma_s^2) [B_{\nu}(T_s) - I_{\nu}^{\downarrow}(\theta)] d\varphi_n d\mu_n}$$

- **Effective emissivity** is the guiding principle behind **cavity blackbodies** (e.g., *Prokhorov 2012*) commonly used for calibration of IR sensors.
 - A cavity’s surface is **not** inherently black
 - However, it is the cumulative effect of emission and reflection off the surface that **enhances the effective emissivity** of the cavity
 - Thus, while the “optical emissivity” of the cavity is non-black, it nevertheless **appears black to the sensor**, which is ultimately all we care about
 - The sensor does **not** discriminate between directly emitted or multiply reflected contributions to the radiance
 - The **same principle holds for any natural rough surface**, including the sea surface — **reflection of radiance effectively enhances the apparent emissivity of the surface**

Derivation of Sea-Surface Effective Emissivity



Then, defining an **effective emissivity** as

$$\mathcal{E}_\nu(\theta_0) \equiv 1 - \rho_\nu[\Theta_e(\theta_0)],$$

where Θ_e is an **effective emission angle**, $\Theta_e \equiv \overline{\Theta}_i - \Delta\Theta_i \lesssim \overline{\Theta}_i$, which compensates residual diffuse reflectance, one may arrive at a **simplified quasi-specular RTE for the SLR**

$$R_{\nu s}(\theta_0) = \mathcal{E}_\nu(\theta_0) B_\nu(T_s) + [1 - \mathcal{E}_\nu(\theta_0)] I_\nu^\downarrow(\theta_0).$$

From this we see the effective emissivity as defined is equivalent to

$$\mathcal{E}_\nu(\theta_0) = \frac{R_{\nu s}(\theta_0) - I_\nu^\downarrow(\theta_0)}{B_\nu(T_s) - I_\nu^\downarrow(\theta_0)}$$

We can derive the effective emission angle Θ_e iteratively via **least-squares spectral minimization** of RMSE

$$\text{RMSE}(\Delta\nu) = \sqrt{\frac{1}{n-1} \sum_\nu [T_{\nu s}(\Theta_e) - T_s]^2},$$

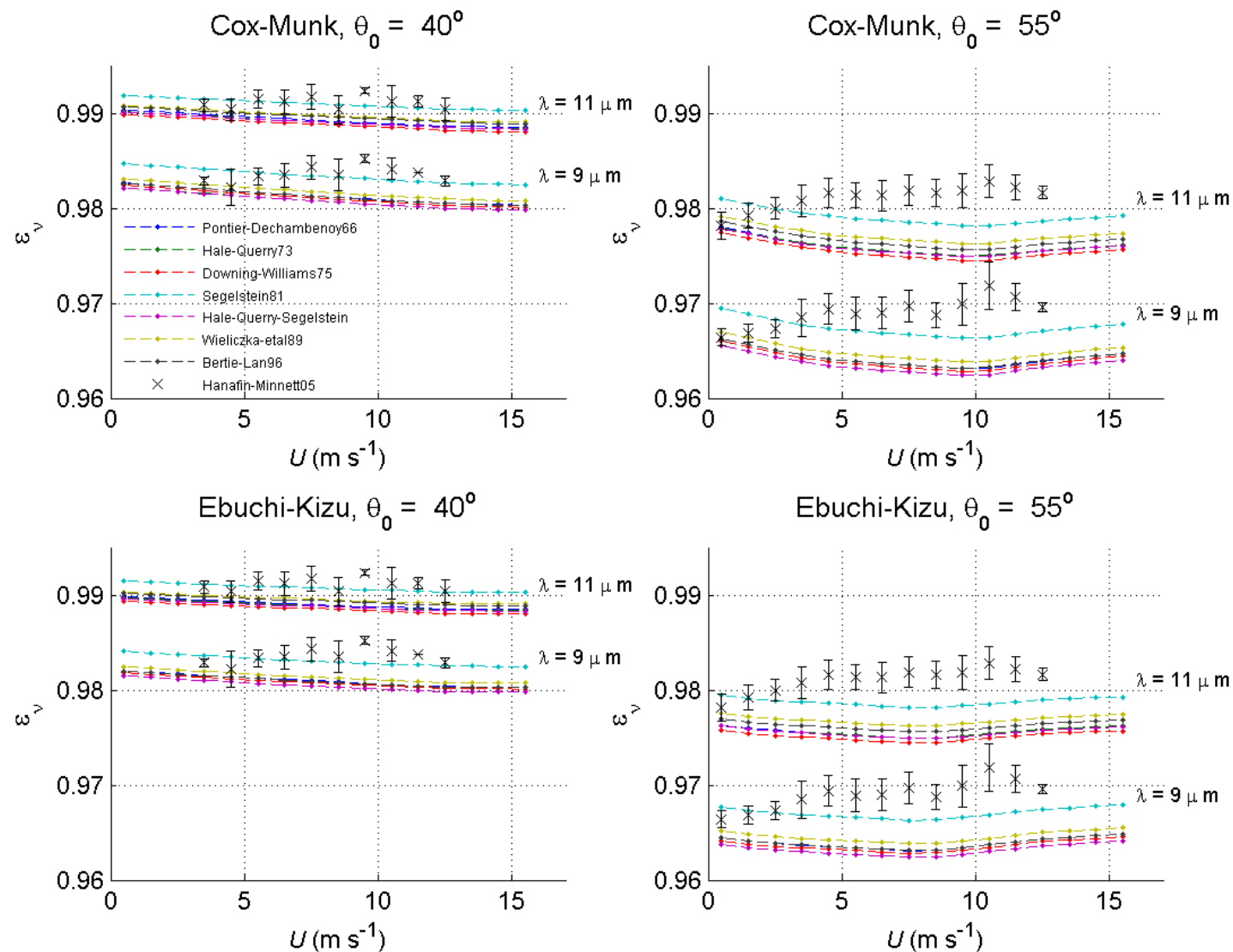
where $T_{\nu s}(\Theta_e)$ is the radiometric skin temperature given by

$$T_{\nu s}(\Theta_e) = B_\nu^{-1} \left(\frac{R_{\nu s}(\theta_0) - \rho_\nu(\Theta_e, N_\nu) I_\nu^\downarrow(\theta_0)}{1 - \rho_\nu(\Theta_e, N_\nu)} \right)$$

The retrieved Θ_e over finite spectral intervals can then be used to derive the entire effective emissivity spectrum.

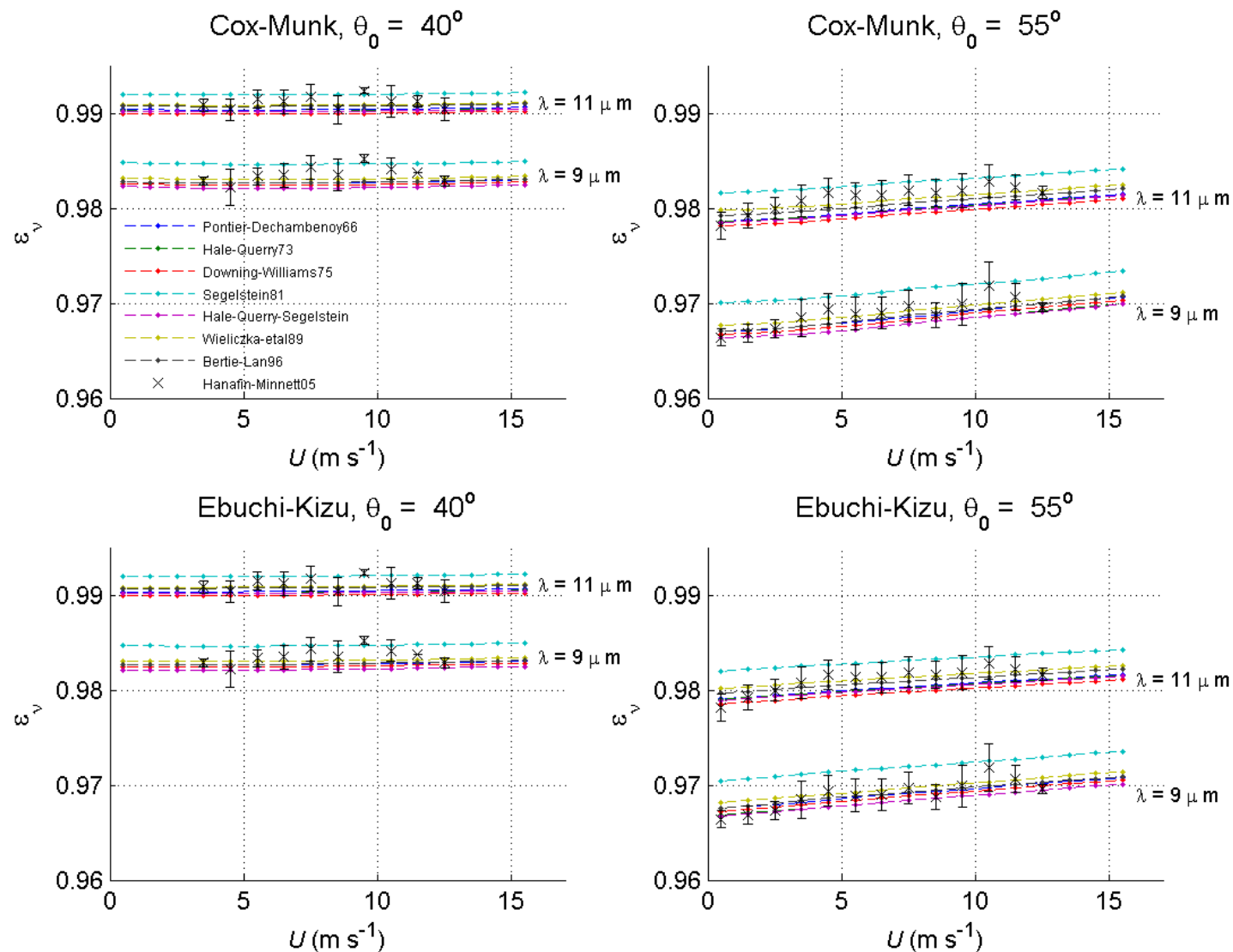
Calculated Emissivity versus MAERI-1 Observation

Masuda (2006) Model vs
Hanafin and Minnett (2005)
MAERI observations



Calculated Effective Emissivity MAERI-1 Observation

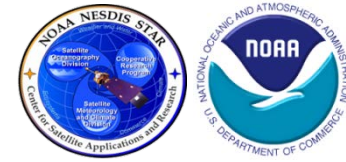
Nalli et al. (2008) IRSSE Model vs
Hanafin and Minnett (2005)
MAERI observations



IR Ocean Emissivity Models

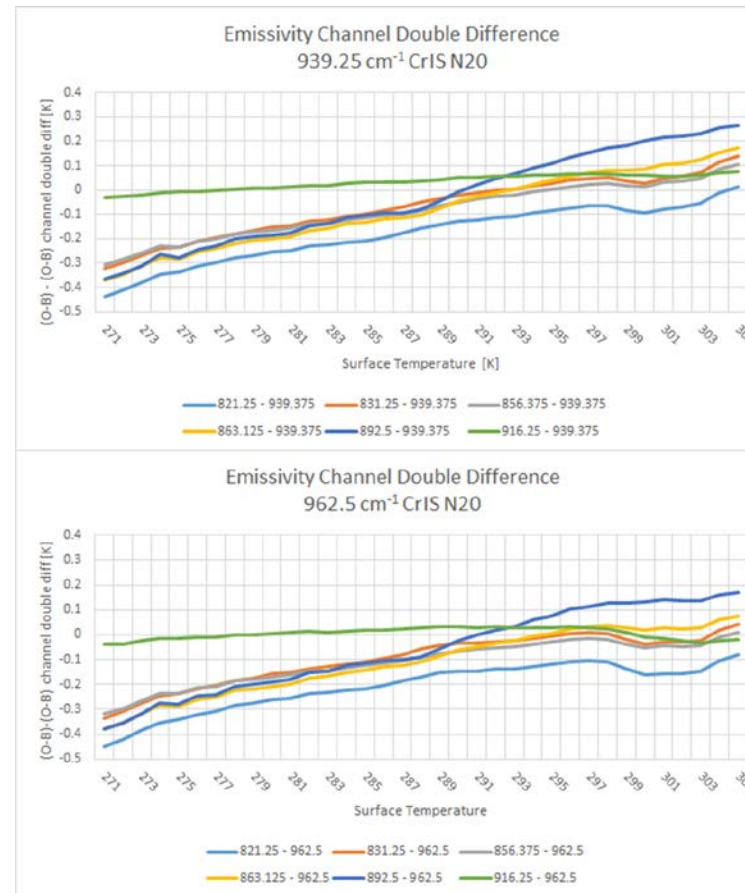
CURRENT TOPICS OF ONGOING RESEARCH

Observed and Modeled Global Scale Impact of Temperature

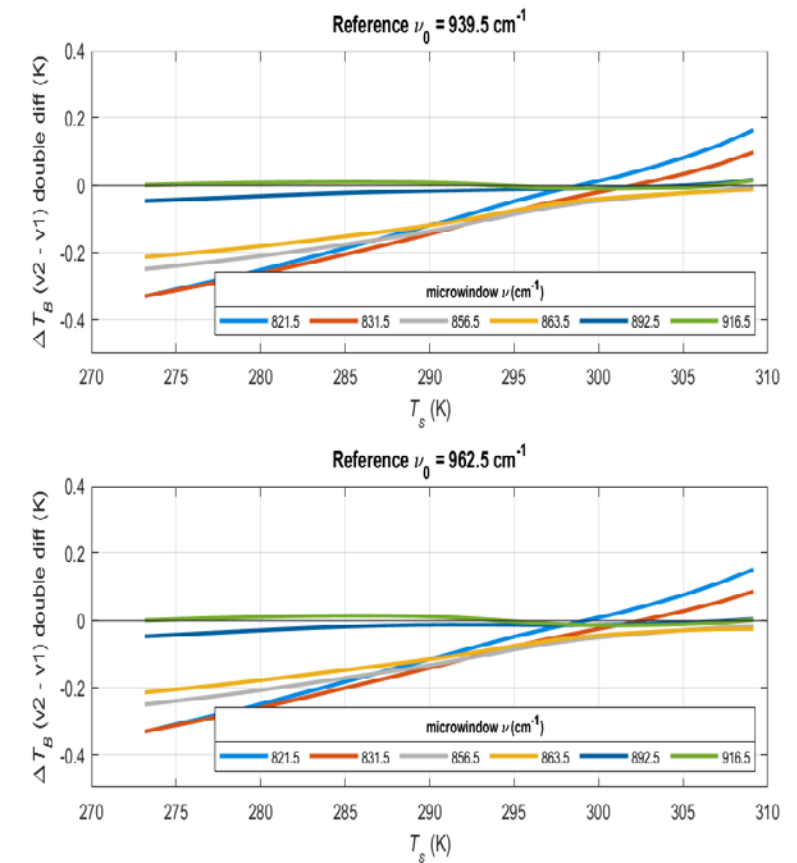


- While it has been known that the IR refractive indices depend on temperature (*Newman et al. 2005*), recent findings (*Liu et al. 2019*) showed a **significant systematic bias (order of 0.5 K) on a global scale**, thus bringing this issue back into focus for support (JCSDA and JPSS)
- **Global OBS – CALC double-differences**
 - 2-weeks global NOAA-20 CrIS data (obs) versus CRTM model calculations (calc)
 - Microwindow double-differences of obs – calc place control on the unknown atmospheric path uncertainties (e.g., model bias, cloud contamination, H₂O errors, etc.)
 - **Significant surface-temperature dependence ≥ 0.5 K** is clearly visible. This is of first order significance within the context of the total forward model uncertainty.

Observed Global Double-Differences



Simulated Global Double-Differences



Temperature-Dependent Optical Constants (1/2)

- An *ad hoc* “**data rescue**” was performed to obtain temperature-dependent water **optical constants** (i.e., complex refractive index) published by *Pinkley et al. (1977)*
 - They tabulated only a **small subset of the IR spectrum** (further truncated to only 3 significant figures), but plotted the full spectrum in two figures (shown on right)
 - Unfortunately, these are the only known temperature-dependent, laboratory-derived data available for the complete IR spectrum
 - Tried to contact the original authors, but without success
 - Therefore, a **high-res image scan** of the hardbound copy (provided by the library) was **digitized** and then **merged** with the tabulated data
 - This is a suboptimal solution, but it is the best we can do under the circumstances

High-Res Scan of Figures 3 and 4 from *Pinkley et al. (1977)*

$$n_\nu \equiv \Re(N_\nu)$$

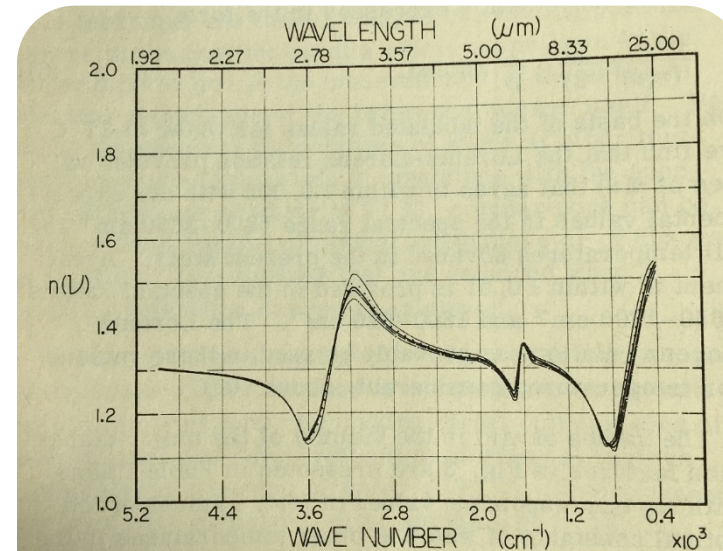


FIG. 3. Refractive index $n(\nu)$ for water at various temperatures: light continuous curve, 1 °C; dotted curve, 16 °C; heavy continuous curve, 27 °C; dashed curve, 39 °C; and dash-dot-dash curve, 50 °C.

$$k_\nu \equiv \Im(N_\nu)$$

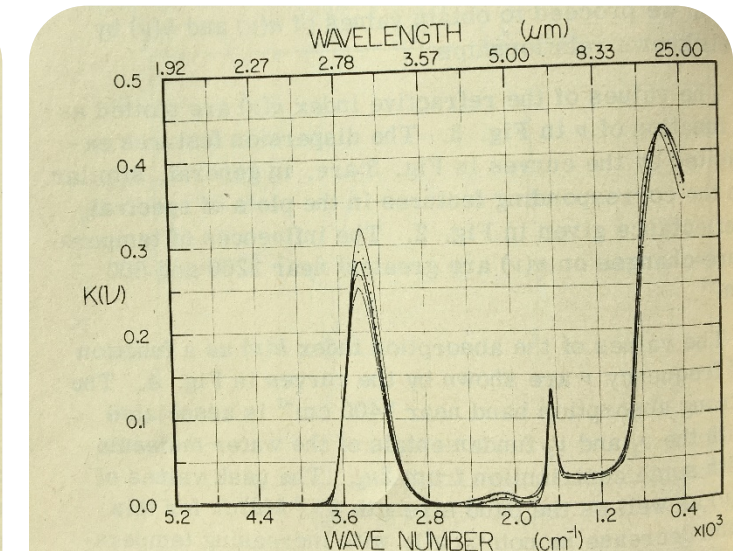
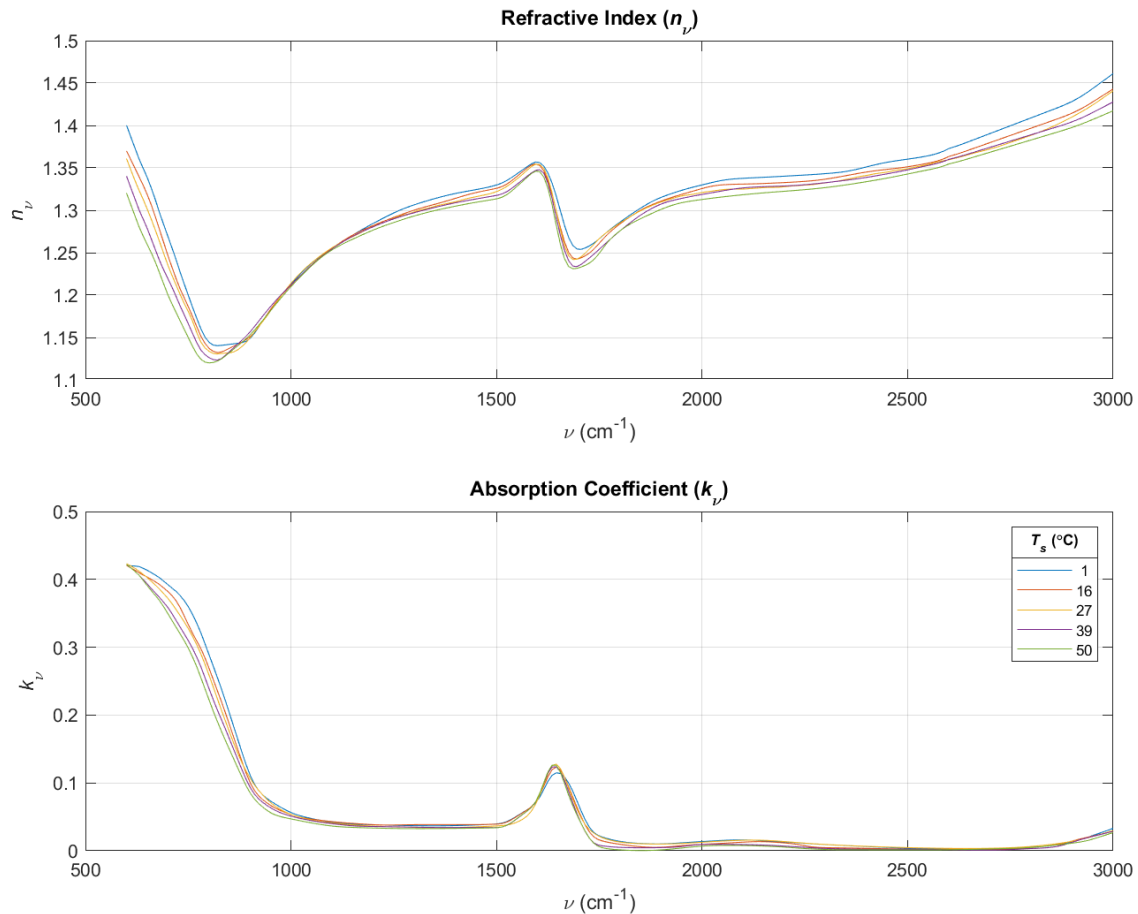


FIG. 4. Absorption index $k(\nu)$ for water at various temperatures: light continuous curve, for 1 °C; dotted curve, 16 °C; heavy continuous curve, 27 °C; dashed curve, for 39 °C; and dash-dot-dash curve, 50 °C.

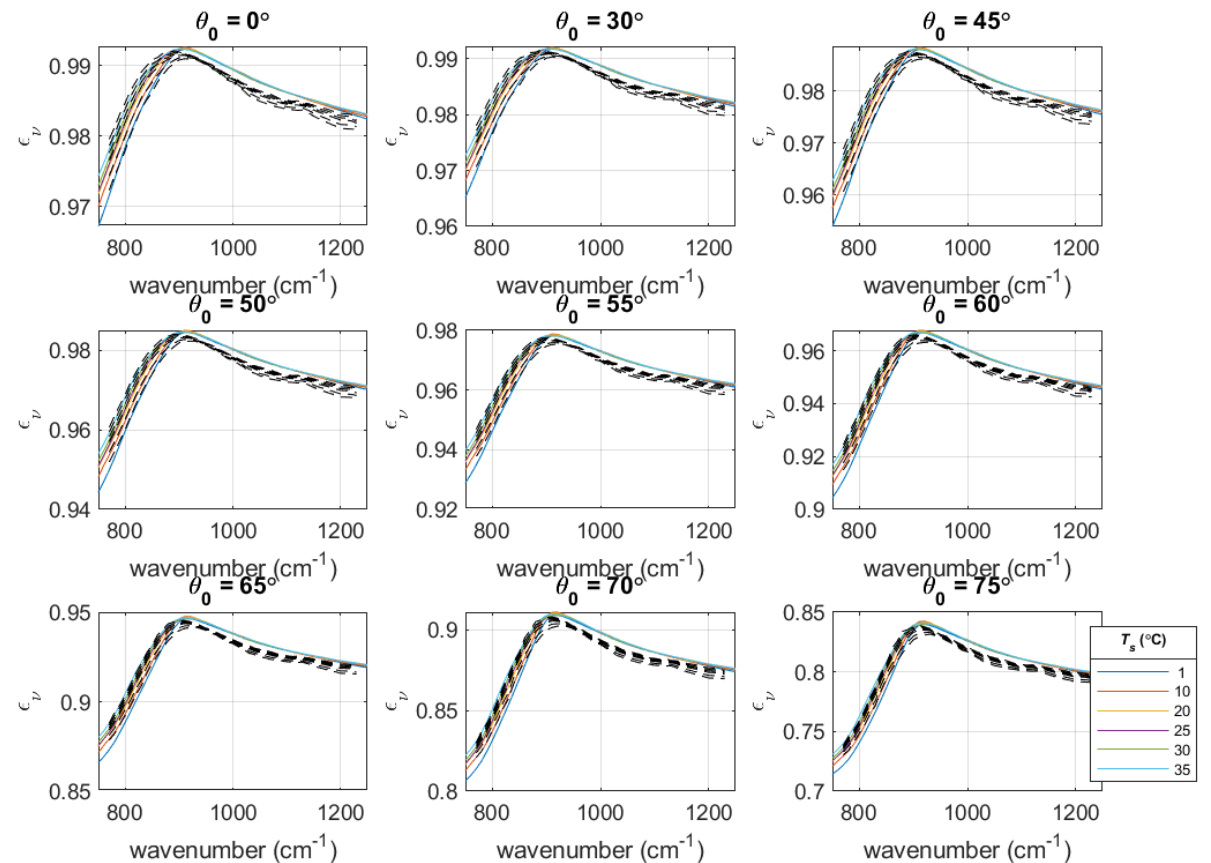
Temperature-Dependent Optical Constants (2/2)

Data Rescue of *Pinkley et al. (1977)* Temperature-Dependent IR Complex Refractive Index N_ν of Water



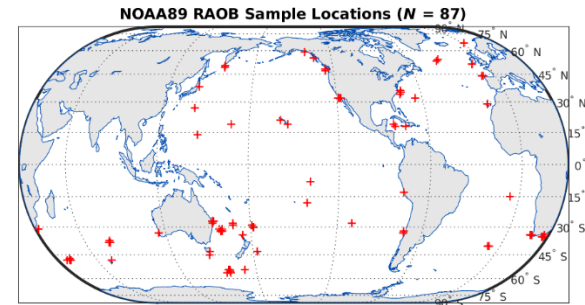
Comparison of Modeled Fresnel Emissivities *Pinkley et al. (1977)* versus *Newman et al. (2005)*

Modeled Fresnel Emissivities from Pinkley (colors) & Newman (black dotted) Ref Ind



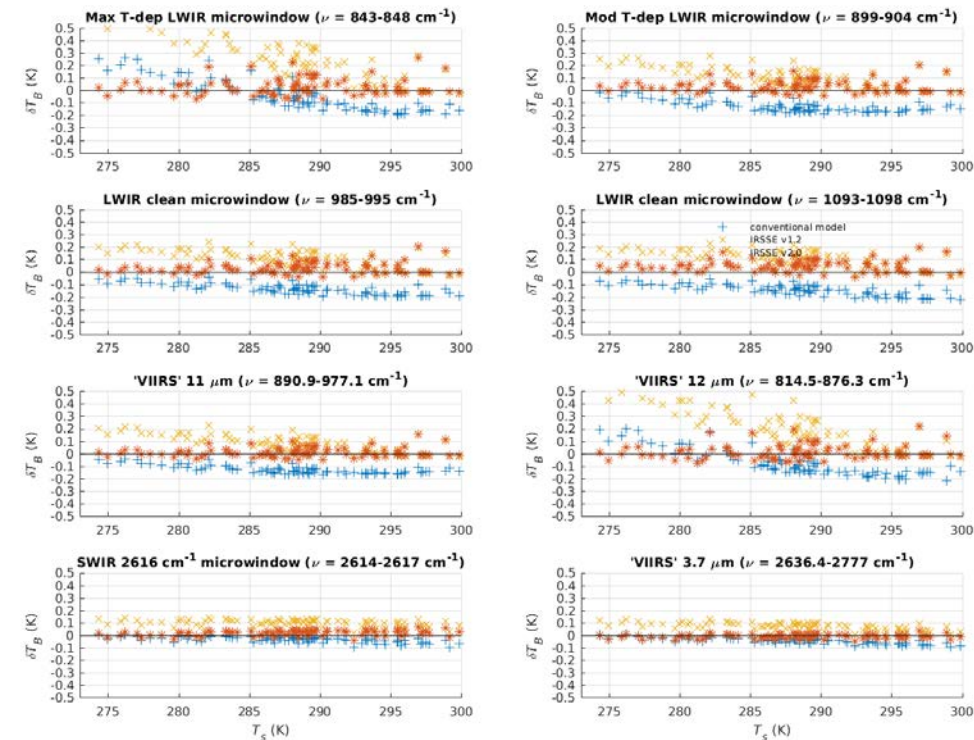
Development and Testing Status

- **Preliminary 4-D lookup tables (LUT)** (including temperature dimension have been generated and are undergoing testing
- **Theoretical testing** of the latest test LUT has been conducted against independent simulated data based on the NOAA89 RAOB dataset
 - The results show improved performance of the IRSSE upgrade versus view angle and surface temperature.
- **Empirical testing** of the adjusted LUT has been conducted versus 2 ship-based campaigns
 - **MARCUS 2017** campaign (Southern Ocean, cold water; data courtesy of Bob Knuteson and Jon Gero, UW/CIMSS)
 - **CSP 1996** campaign (Tropical Western Pacific Warm Pool; *Post et al.* 1997)

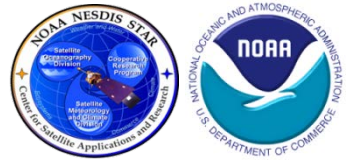


Conventional model (*Masuda 2006*)
 CRTM IRSSE v1.2 (*Nalli et al.* 2008)
 CRTM IRSSE v2.0 Test

NOAA89 RAOB $N=87$; $U=10$ m/s; Ebuchi-Kizu; Pinkley-eta177; $\theta=55^\circ$



Marine Atmospheric Emitted Radiance Interferometer (MAERI)



- **Ship-based FTS** designed to sample downwelling and upwelling IR high-resolution spectra near the surface (*Minnett et al. 2001*)
 - Original prototypes designed at **UW/SSEC**
 - First generation MAERIs were supported and deployed by **UM/RSMAS**
 - Second generation MAERIs have recently been developed and deployed by both UM/RSMAS and the **ARM Mobile Facility 2 (AMF2)**
- **High accuracy calibration** (e.g., *Revercomb et al. 1988*) is achieved using 2 NIST-traceable blackbodies
- **Radiometric skin SST** (0.1 K accuracy) derived from semi-opaque spectral region ($\approx 7.7 \mu\text{m}$) (*Smith et al. 1996*)

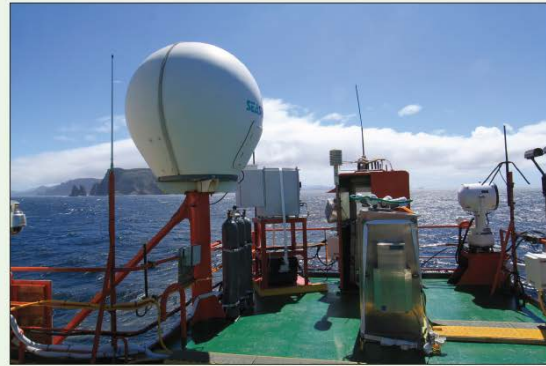
ARM Mobile Facility (AMF2) MAERI
2015 CalWater/CAPEX



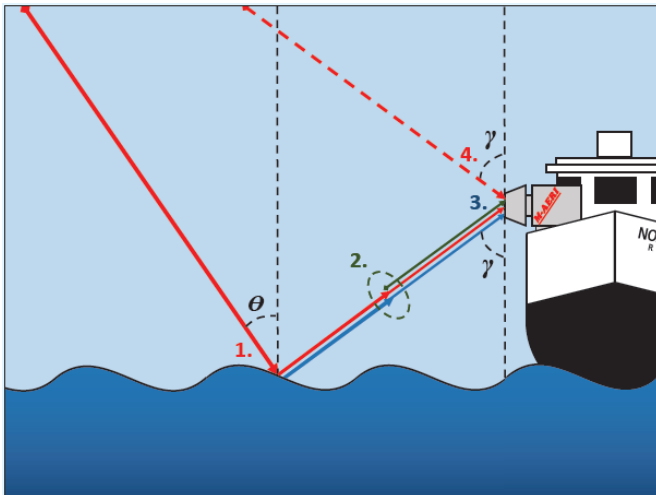
UM/RSMAS MAERI
Routinely deployed during AEROSE

Cold-Water MAERI Data Analysis

Measurements of Aerosols, Radiation, and Clouds over the Southern Ocean (MARCUS)



DOE ARM Marine-AERI (ABB/UW-SSEC)

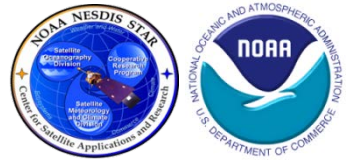


- The DOE **ARM Mobile Facility** was deployed on the Australian Icebreaker *Aurora Australis* with 3 roundtrip transits between Hobart, Tasmania and research stations along the Antarctic coast, Oct 2017 – Mar 2018
 - DOE AMF includes **MAERI** built by ABB under license from UW/SSEC
- High quality radiance observations were obtained 4 oblique angles of the ocean surface and atmosphere
- The transits sampled a range of skin temperatures, 273–287K, and wind speeds, 0–25 m/s
- Emissivities derived from the MAERI data indicate a temperature dependence similar that hypothesized

Courtesy of Bob Knuteson and Jon Gero (UW/CIMSS)

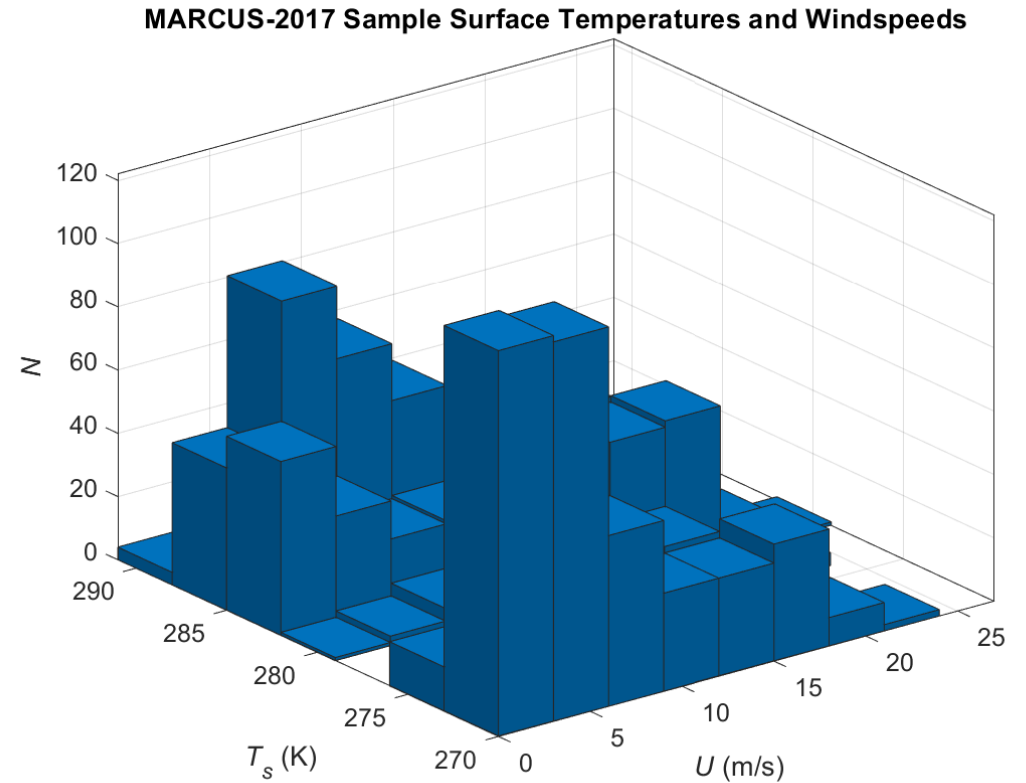
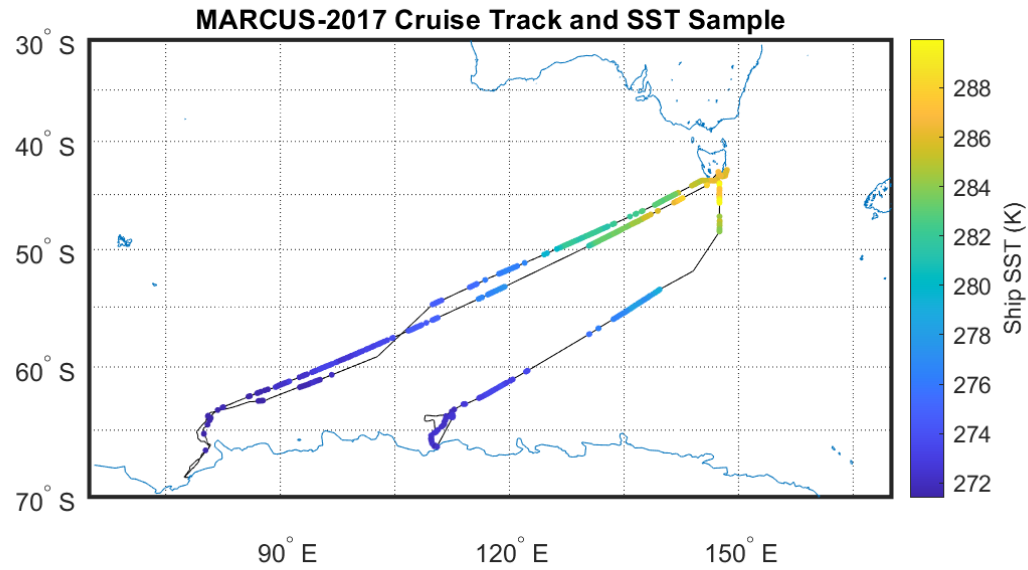
<https://www.arm.gov/research/campaigns/amf2017marcus>

MARCUS Sample Overview

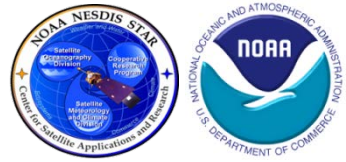


MARCUS Cruise Track and Ship Intake SST

Histogram of Surface Temperatures and Windspeeds



SST-Binned Mean LWIR Spectra ($\theta_0 = 55^\circ$)



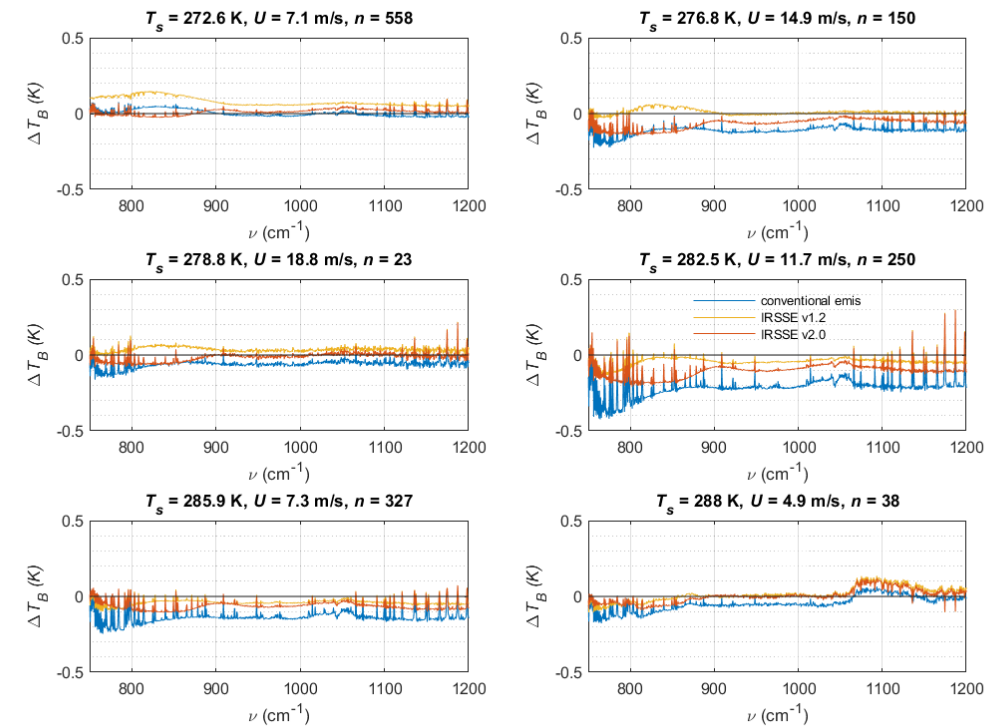
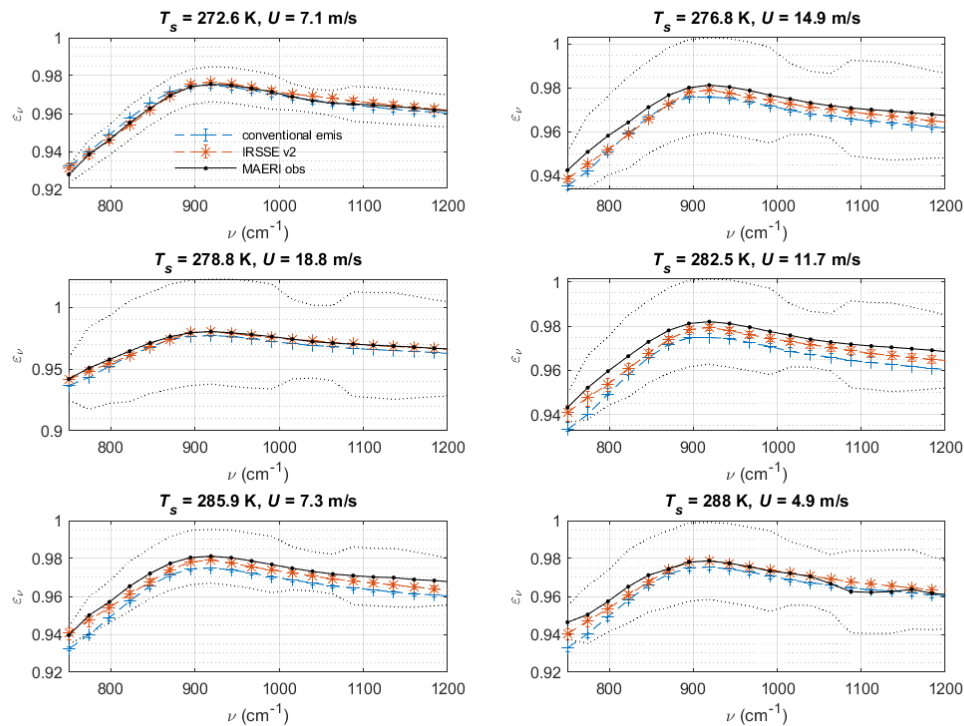
Conventional model (*Masuda 2006*)
 CRTM IRSSE v1.2 (*Nalli et al. 2008*)
 CRTM IRSSE v2.0 Test

Emissivities

calc – obs

MARCUS-2017 LWIR Emissivities, $\theta_0 = 55^\circ$

MARCUS-2017 LWIR calc-obs, $\theta_0 = 55^\circ$



SST-Binned Mean LWIR Spectra ($\theta_0 = 60^\circ$)



Conventional model (*Masuda 2006*)

CRTM IRSSE v1.2 (*Nalli et al. 2008*)

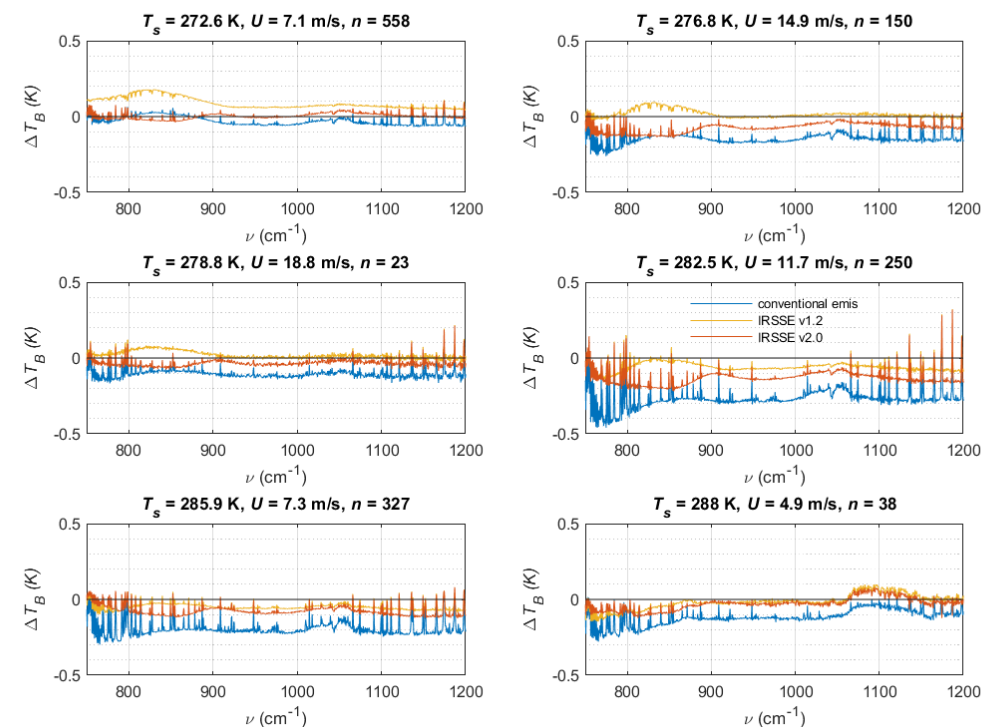
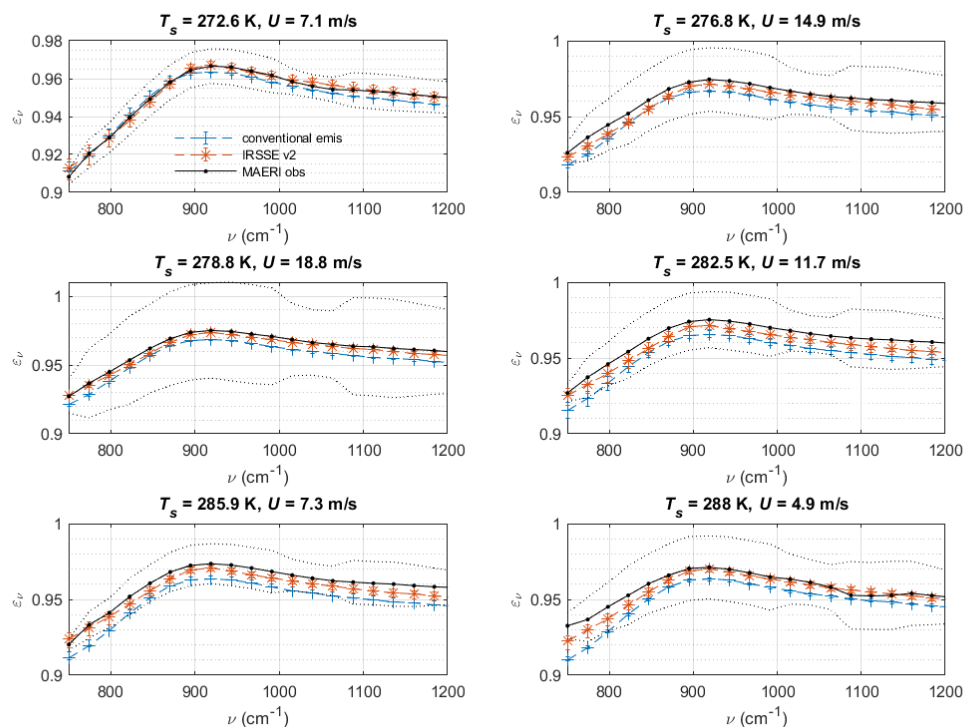
CRTM IRSSE v2.0 Test

Emissivities

calc - obs

MARCUS-2017 LWIR Emissivities, $\theta_0 = 60^\circ$

MARCUS-2017 LWIR calc-obs, $\theta_0 = 60^\circ$



SST-Binned Mean LWIR Spectra ($\theta_0 = 65^\circ$)



Emissivities

Conventional model (*Masuda 2006*)

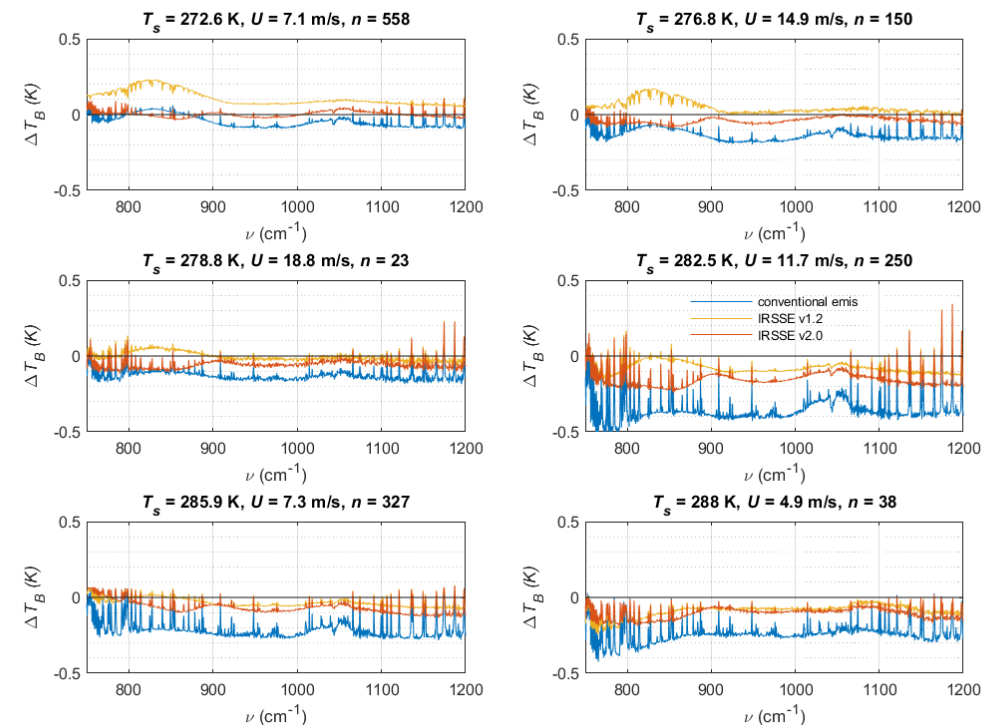
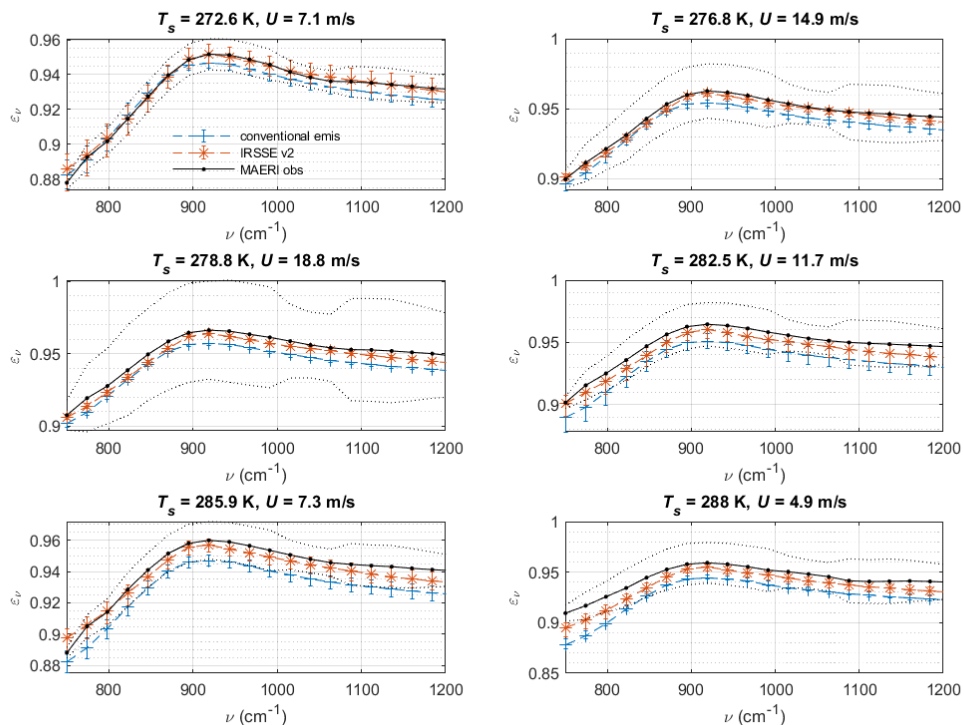
CRTM IRSE v1.2 (*Nalli et al. 2008*)

CRTM IRSE v2.0 Test

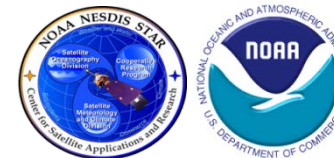
calc – obs

MARCUS-2017 LWIR Emissivities, $\theta_0 = 65^\circ$

MARCUS-2017 LWIR calc-obs, $\theta_0 = 65^\circ$



SST-Binned Mean LWIR Spectra ($\theta_0 = 70^\circ$)



Emissivities

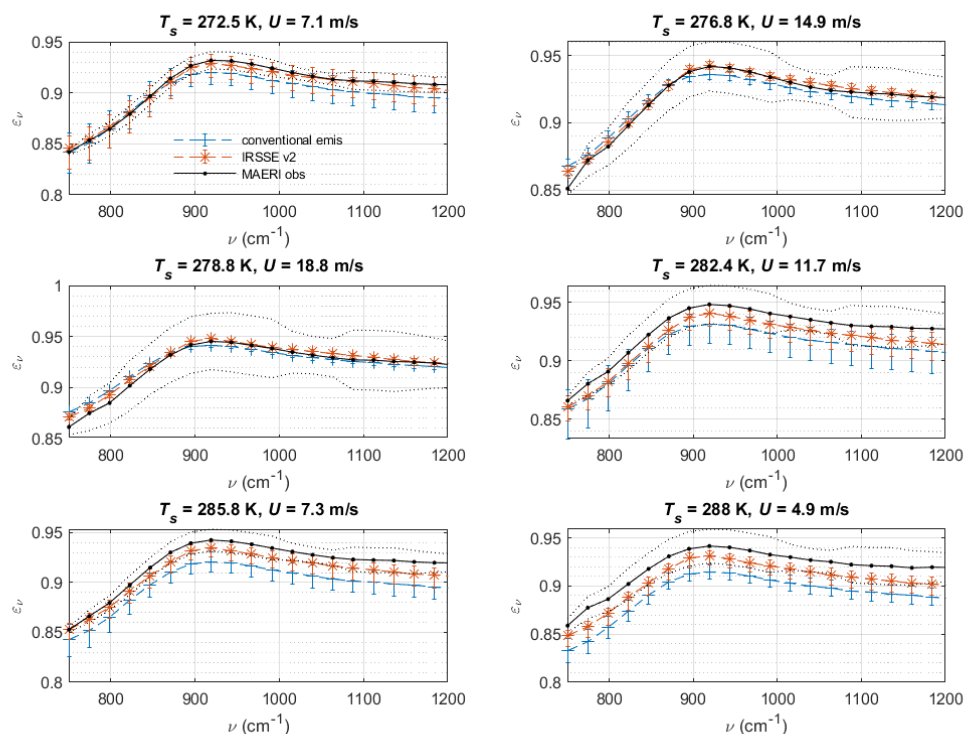
Conventional model (*Masuda 2006*)

CRTM IRSSE v1.2 (*Nalli et al. 2008*)

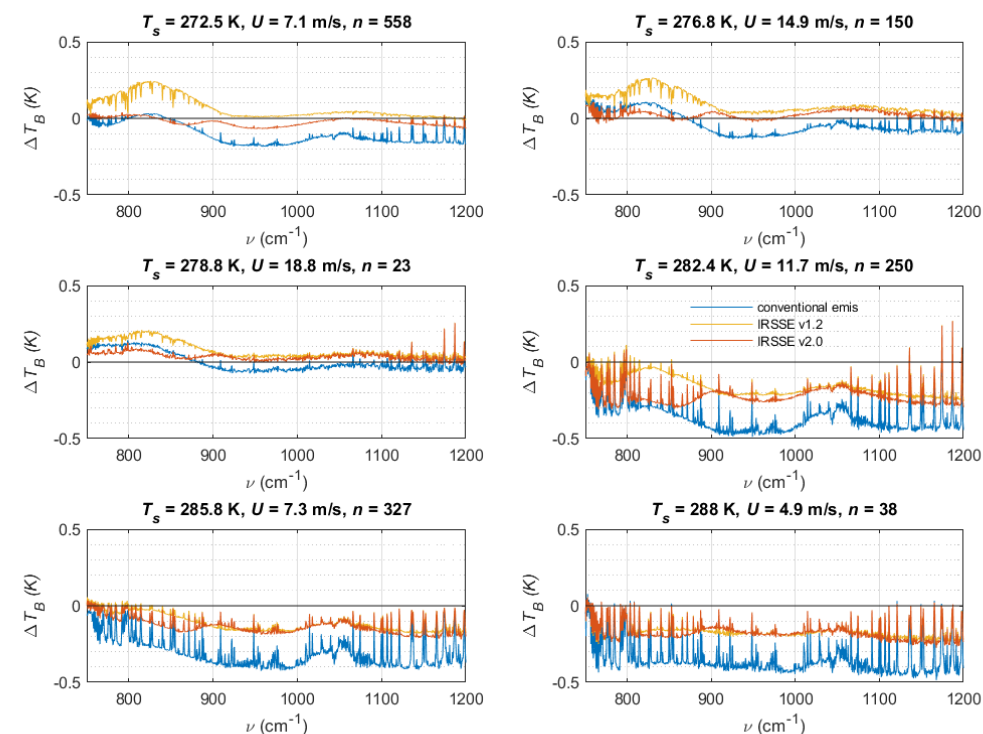
CRTM IRSSE v2.0 Test

calc – obs

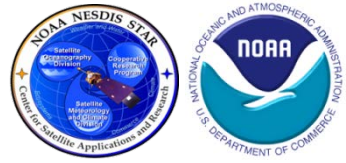
MARCUS-2017 LWIR Emissivities, $\theta_0 = 70^\circ$



MARCUS-2017 LWIR calc-obs, $\theta_0 = 70^\circ$



LWIR Split-Window Trend Analysis vs SST



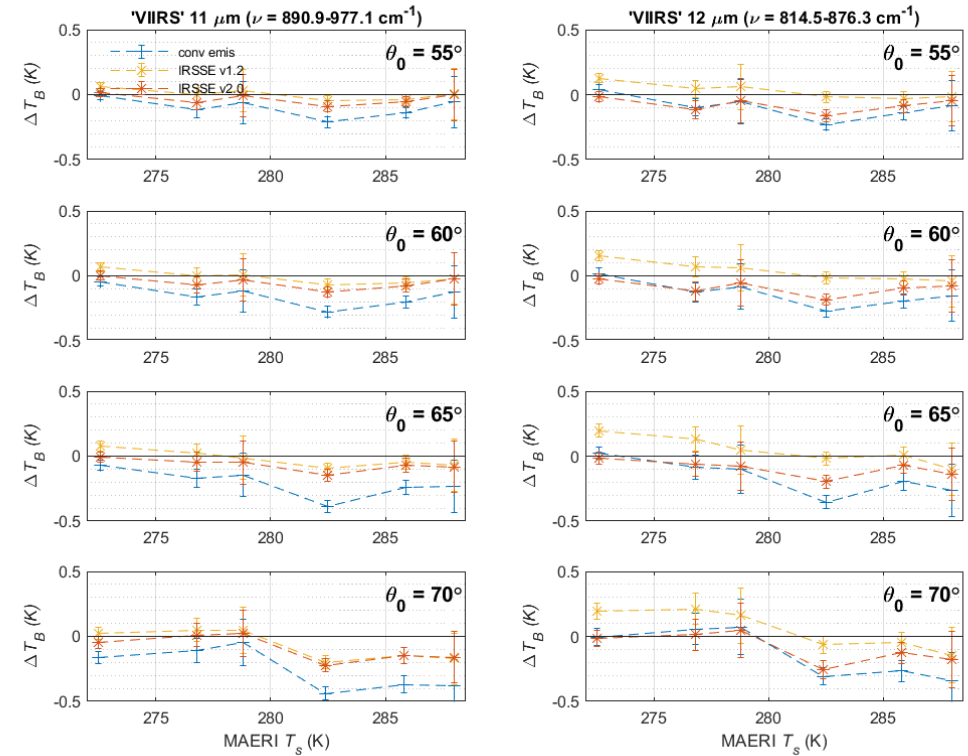
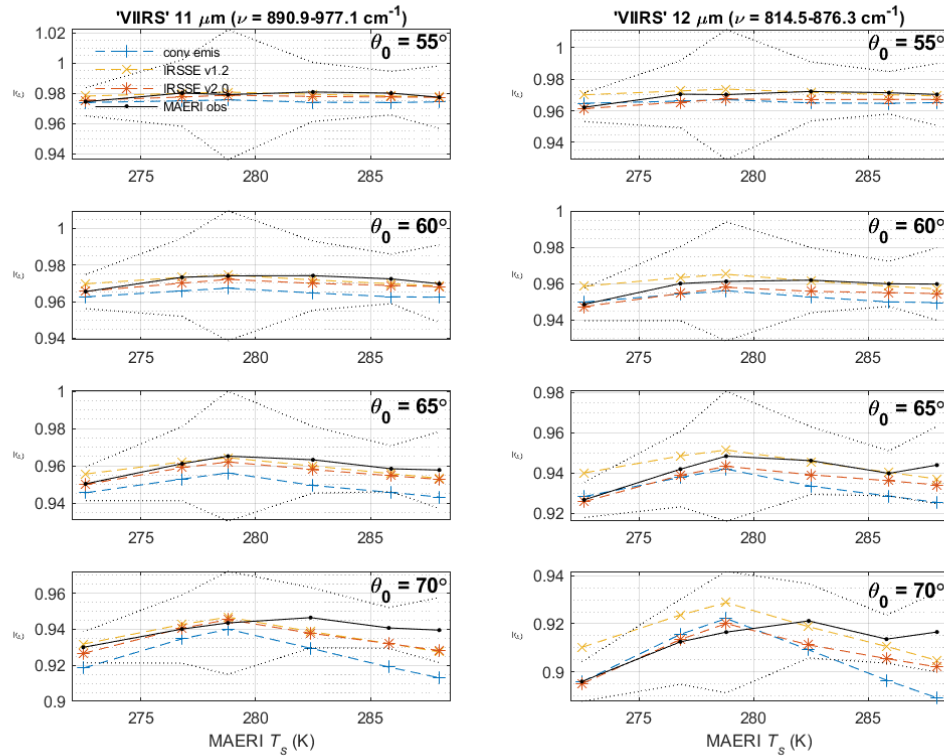
Conventional model (*Masuda 2006*)
 CRTM IRSE v1.2 (*Nalli et al. 2008*)
 CRTM IRSE v2.0 Test

Emissivities

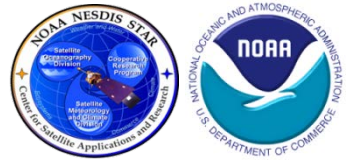
calc – obs

MARCUS-2017 LWIR Split-Window Emis vs SST

MARCUS-2017 LWIR Split-Window calc-obs vs SST



MAERI Results Summary



- **calc – obs** of the IR surface-leaving radiance (SLR) is a preferred metric for assessing model performance
 - **MAERI directly measures SLR** (neglecting path absorption) along with the downwelling atmospheric radiance at the corresponding zenith angle
 - This allows for direct assessment of the IRSSE model as it pertains to the CRTM and most IR SLR forward models
- The **MARCUS** and **CSP** campaigns included a significant sample of cold, intermediate and warm water cases
 - MAERI was specially configured for the emissivity/SLR application by viewing the surface and atmosphere at varying oblique view angles
 - MARCUS campaign: 55°, 60°, 65°, 70°
 - CSP campaign: 35°, 45°, 55°, 65°
- The **IRSSE v2.0 test LUT** exhibits good overall agreement with the MAERI observations at over the range of surface temperature and windspeeds
 - Known systematic spectral biases ($\approx 0.1\text{--}0.5$ K) associated with surface temperature dependence and the ocean BRDF are significantly reduced versus MAERI observations as compared to “conventional models” (e.g., *Masuda 2006*), as well as the IRSSE v1.2 (currently in CRTM)
 - Additional MAERI validation campaigns are desirable
 - *Ebuchi & Kizu* PDF slopes appear to yield better agreement at low windspeeds
 - Additional work testing the test model within operational GSI assimilation and SARTA implementation is ongoing

Upcoming Work



- Additional confidence in the IRSSE v2.0 could be obtained from additional empirical testing versus MAERI datasets
 - **2015 CalWater/ACAPEX campaign** (midlatitude Pacific)
 - Would need to obtain these data from UW/CIMSS
 - Other campaigns as time allows
- An **offline CRTM version** has been made available to Jim Jung et al. for **global obs – calc (GFS/CRTM) impact analysis**
 - Currently seeing positive impact in channels below from 800–890 cm^{-1} , but there appears to be lingering T-dependence from 890–925 cm^{-1} , likely due to limitations in the *ad hoc* Pinkley optical constants
 - Still ironing out issues elsewhere, e.g., in the window border region of 750–800 cm^{-1}
- **SARTA implementation** requires modification of the “Reflected Downwelling Thermal Radiance” term
 - According to *Strow et al. (2003)*, an **approximation** is used (based on *Kornfield & Susskind 1977*) that may “require further improvements”:
$$r_v(\theta) \approx \pi \rho_v^F B_v(T_v) [1 - T_{vs}(\theta)] F_v(\theta)$$
 - Currently looking into upgrading the “Reflected Downwelling” Lambertian approximation within SARTA over oceans to implement the IRSSE with temperature dependence)
 - NUCAPS SST analyses have been devised in support of a future SARTA model impact analysis
- **Ultimately, a new set of laboratory-measured IR optical constants of water would be highly desirable for this effort**



IR Ocean Emissivity Models

THANK YOU! QUESTIONS?



IR Ocean Emissivity Models

BACKUP SLIDES